HHS Public Access

Author manuscript

Neuroimage. Author manuscript; available in PMC 2019 May 02.

Published in final edited form as:

Neuroimage. 2018 December ; 183: 327–335. doi:10.1016/j.neuroimage.2018.08.020.

Optimal referencing for stereo-electroencephalographic (SEEG) recordings

Guangye Li[a,e,2], **Shize Jiang**[b,2], **Sivylla E. Paraskevopoulou**[e,2], **Meng Wang**[a], **Yang Xu**[a], **Zehan Wu**[b], **Liang Chen**[b,**,1], **Dingguo Zhang**[a,*,1], and **Gerwin Schalk**[c,d,e]

[a]State Key Laboratory of Mechanical Systems and Vibrations, Institute of Robotics, Shanghai Jiao Tong University, Shanghai, China

[b]Department of Neurosurgery of Huashan Hospital, Fudan University, Shanghai, China

[c]Department of Biomedical Sciences, State University of New York, Albany, NY, USA

[d]Department of Neurology, Albany Medical College, Albany, NY, USA

[e]National Center for Adaptive Neurotechnologies, Wadsworth Center, New York State Department of Health, Albany, NY, USA

Abstract

Stereo-electroencephalography (SEEG) is an intracranial recording technique in which depth electrodes are inserted in the brain as part of presurgical assessments for invasive brain surgery. SEEG recordings can tap into neural signals across the entire brain and thereby sample both cortical and subcortical sites. However, even though signal referencing is important for proper assessment of SEEG signals, no previous study has comprehensively evaluated the optimal referencing method for SEEG. In our study, we recorded SEEG data from 15 human subjects during a motor task, referencing them against the average of two white matter contacts (monopolar reference). We then subjected these signals to 5 different re-referencing approaches: common average reference (CAR), gray-white matter reference (GWR), electrode shaft reference (ESR), bipolar reference, and Laplacian reference. The results from three different signal quality metrics suggest the use of the Laplacian re-reference for study of local population-level activity and low-frequency oscillatory activity.

Keywords

Stereo-electroencephalography; SEEG; Referencing method; Signal quality; Noise subtraction

[*]Corresponding author. [**]Corresponding author.

[1]Co-corresponding authorship.

[2]Contribute to this paper equally and should be considered as co-first authors.

Appendix B. Supplementary data

Supplementary data related to this article can be found at https://doi.org/10.1016/j.neuroimage.2018.08.020

1. Introduction

Intracranial recordings have been employed in humans clinically for over six decades for the localization of epileptic zones and for functional brain mapping. However, their unique value for basic human neuroscientific research and their potential for enabling new translational applications has only been widely recognized for the past several years.

Up to the present, the most common technique for acquiring intracranial data has been electrocorticography (ECoG). In this modality, circular electrodes (of usually 2–3 mm diameter and with 5–10 mm spacing) are placed directly on the lateral surface of the cortex. Many studies over the last two decades have demonstrated the high functional specificity (Leuthardt et al., 2004; Schalk et al., 2007), signal fidelity (Ball et al., 2009), and long-term stability (Schalk, 2010; Chao et al., 2010; Nurse et al., 2018) of ECoG activity (but see Ung et al. (2017)). Together with its high spatial resolution (Freeman et al., 2000; Slutzky et al., 2010) and temporal resolution, and coverage of distant areas of the brain, these unique qualities suggest that ECoG can elucidate brain function in ways that cannot be achieved by other electrophysiological or neuroimaging techniques.

Stereo-encephalography (SEEG) is a different intracranial technique. Instead of placing electrodes on the lateral surface of the cortex, SEEG inserts depth electrodes into the human brain. These electrodes usually contain multiple recording contacts (typically 8–16 contacts with a 3.5 mm center-to-center distance) along each electrode's shaft. Signals recorded using SEEG have high amplitude (typically 50–1500 μV), high spatial resolution (typically 3.5 mm) and produce changes across a wide range of frequencies (up to 500 Hz, Urrestarazu et al. (2007)). More importantly, unlike ECoG, which is restricted to cortical recordings, SEEG can record information from both cortical and subcortical structures simultaneously, e.g., white matter (Mercier et al., 2017), hippocampus (Zhang and Jacobs, 2015), basal ganglia (Rektor et al., 2003), or even the thalamus (Rektor et al., 2001). Unlike ECoG, which is usually used clinically to localize seizure foci as well as important functions, SEEG is primarily used as part of a specialized approach to seizure localization tailored to each patient's clinical profile (Chabardes et al., 2017).

SEEG technology was introduced over half a century ago (Bancaud and Talairach, 1965, 1973). Because of the smaller surgical trauma (burr holes instead of a full craniotomy (Sperling and Connor, 1989; Lang and Chitale, 2016)), and because of recent advances in surgical robotics (Cardinale et al., 2016), SEEG has become increasingly prevalent in clinical practice (Munari et al., 1994; Ayoubian et al., 2010; Cossu et al., 2005; Guenot et al., 2001; Lachaux et al., 2003; Proserpio et al., 2011; Ryvlin and Picard, 2017). In addition to potential clinical benefits, SEEG also opens a unique window into brain function, because it can sample the temporal evolution of neural activity at many locations throughout the brain (Jerbi et al., 2009; Koessler et al., 2010; Lachaux et al., 2006; Lakatos et al., 2007; Perrone-Bertolotti et al., 2012; Vidal et al., 2012).

Just like ECoG and unlike EEG, SEEG can detect two of the most important features of intracranial recordings, broadband gamma activity and low-frequency oscillatory activity. Many studies have shown that broadband gamma activity (signal amplitude at frequencies

larger than 60 Hz) is a reliable indicator of population-level cortical activity related to different motor, sensory, or cognitive tasks (Gaona et al., 2011; Ray and Maunsell, 2011; Potes et al., 2014; Miller et al., 2014; de Pesters et al., 2016; Branco et al., 2017). In contrast to broadband gamma, low-frequency oscillatory activity is thought to modulate cortical excitability (Schalk et al., 2017) and the performance of resulting behavior (Coon et al., 2016). Because low oscillatory power indexes high cortical excitability, broadband gamma activity is usually higher for decreased oscillatory power (Haegens et al., 2011; Klimesch, 2012; Schalk, 2015; Schalk et al., 2017; Jensen and Mazaheri, 2010).

Detection of broadband gamma and oscillatory activity begins by first referencing a signal at a particular location against the signal at one or two reference location(s) during recording, and then applying, usually in post-hoc analyses, a specific re-referencing method. The choice for referencing locations usually follows specific guidelines (Landré et al., 2018), and optimization of that choice may lead to distinct advantages (Mercier et al., 2017). The benefits and shortcomings of different re-referencing techniques have been determined for ECoG (Liu et al., 2015), but not yet for SEEG (but see Mercier et al. (2017)). The optimal re-referencing for SEEG may differ from that for ECoG, because SEEG samples across different structures in the brain (e.g., cortex and white matter) that may have different amplitude, impedance, or other characteristics. In the present study, we systematically evaluate the effect of six different referencing methods on the raw signal, broadband gamma, and oscillatory power of SEEG recordings during a motor task. The results show that the use of a local Laplacian derivative minimizes inter-channel correlation and maximizes correlations with the task.

2. Materials and methods

2.1. Subjects and data recording

Fifteen right-handed subjects participated in this study. The subjects were patients with intractable epilepsy who had SEEG electrodes implanted for pre-surgical assessment of their seizure focus. The clinical profile of the subjects is shown in Table 1. All implant parameters were solely determined by clinical needs rather than the needs of our research. SEEG signals were acquired using a clinical recording system (EEG-1200C, Nihon Kohden, Irvine, CA) and sampled with 500–2000 Hz. We also recorded electromyographic (EMG) signals from the extensor carpi radialis muscle using two surface EMG electrodes. EMG was simultaneously recorded using the same amplifier and the same sampling rate as the SEEG signals. All subjects gave informed consent for this study, which was approved by the Ethics Committee of Huashan Hospital (Shanghai, China).

2.2. Experimental protocol

The experimental task is shown in Fig. 1. The subjects were visually cued to perform 5 types of finger and arm movements. Subjects rested for 4 s before a cue (black cross) appeared on an LCD screen to prepare them for the upcoming movement. After 1 s, a picture of the desired gesture appeared, which prompted the subject to execute that movement. They performed the indicated movement for 5 s until the movement cue disappeared. Thus, each trial lasted 10 s (4 s rest, 1 s cue, 5 s movement). The subjects executed each of the 5

movement types 20 times, resulting in a total of 100 trials per subject (16.67 min total). The type of movement in each trial was randomized. The subjects used the hand contralateral to the hemisphere with the majority of the implanted SEEG electrodes.

2.3. Electrode localization

The 15 subjects had a total of 161 electrode shafts (rounded mean ± std: 11 ± 3 per subject) and 2151 contacts (rounded mean ± std: 143 ± 41 per subject) implanted. Each electrode shaft was 0.8 mm in diameter and contained 8–16 contacts (contact length was 2 mm), and contacts were spaced 3.5 mm center-to-center. We identified the location of all contacts in each individual brain model using pre-surgical MRI, post-surgical CT images, Freesurfer software (http://surfer.nmr.mgh.harvard.edu), and the NeuralAct toolbox (Kubanek and Schalk, 2015). In addition to the coordinates, we identified for each contact the anatomical location (e.g., gray matter, white matter, amygdala, hippocampus) using Freesurfer's cortical parcellation and subcortical segmentation (Desikan et al., 2006; Fischl et al., 2002). Finally, we projected the contacts from each subject onto a standard brain model (Montreal Neurological Institute (MNI)). The location of the contacts and an illustration of how electrode shafts penetrate through different anatomical areas are shown in Fig. 2.

2.4. Referencing methods

For signal recording, SEEG signals were referenced against the average of two white matter contacts that were adjacent to each other and located remotely from the suspected epileptogenic foci and gray matter; this referencing technique was the same for all channels and is commonly used by the surgeons at Huashan hospital, similar to Landré et al. (2018). We will refer to this technique as monopolar reference throughout this work. We evaluated five additional re-referencing methods: common average reference (CAR), gray-white matter reference (GWR), electrode shaft reference (ESR), bipolar reference, and Laplacian reference.

For CAR, SEEG signals were re-referenced to the average of all channels, similar to ECoG studies (Gaona et al., 2011; Kubanek et al., 2009; Schalk et al., 2017). For GWR, we re-referenced each channel that was located in the gray or white matter to the corresponding average of all gray and white matter channels. (We did not re-reference the 9.7% of channels that were located in subcortical structures.) For ESR, we re-referenced each channel to the average signal of all channels on the same shaft.

Bipolar re-referencing has been used in previous SEEG studies, both for clinical (Allen et al., 1992; Kobayashi et al., 2009) and research (Vidal et al., 2012; Zaveri et al., 2006) purposes. To compute the bipolar re-reference, each channel was re-referenced to its adjacent channel on the same electrode shaft. The Laplacian is one of the most widely-adopted re-referencing methods and is often used with EEG and local field potentials (LFPs) recorded with micro-electrode arrays (McFarland et al., 1997; He et al., 2008; Nunez and Westdorp, 1994; Shirhatti et al., 2016). To compute the Laplacian, each channel was re-referenced to the mean value of its two adjacent contacts along the electrode shaft.

For each of these methods, the re-referenced signal S'_i is described by Eq. (1), where u are the contacts used for referencing and $1 \ldots N$ indicates the contact group from which u is

accumulated. The contact group differed for each referencing method, as presented in Table 2. For the channels located at the top and bottom of the electrode shaft, we reduced the equation for the Laplacian to $S'_i = S_i - S_{i-1}$ and $S'_i = S_i - S_{i+1}$, respectively. The channels that were located at the top of the electrode shaft (i.e., closest to the brain surface) were removed from further calculations in the bipolar re-reference.

$$S'_i = S_i - \frac{1}{N} \cdot \sum_{u=1}^{N} S_u \quad (1)$$

2.5. Signal pre-processing

We removed all channels with excessive line noise from our analyses. To identify these channels, we first calculated a measure of line noise (LN) for each channel. Specifically, we applied, at each recording channel, a 2^{nd} order IIR peak filter (MATLAB™ iirpeak function) at 50 Hz (i.e., a filter used to retain the 50 Hz frequency component). The output signal was X_{LN}, and $LN = mean(X_{LN}^2)$. To calculate a cut-off threshold for noisy channels, we concatenated the filtered signals from all channels of each subject. The concatenation output was X_{LN-all}, and the threshold was set at $median(X_{LN-all}) + 10 \cdot mad(X_{LN-all})$, where mad was the mean absolute deviation. Channels whose LN exceeded the threshold were discarded. This procedure eliminated 17 out of the total of 2151 channels from further analyses.[3]

For all remaining channels, we high-pass filtered the raw SEEG signal at 0.5 Hz using a 4th order Butterworth filter to remove slow signal drifts, and then applied the respective re-referencing method as described above.

After re-referencing, we computed activity in the alpha (8–12 Hz) and broadband gamma (60–140 Hz) bands. To do this, we band-pass filtered the signals at those frequencies using a 6th order Butterworth filter. We then extracted alpha and broadband gamma power by computing the squared absolute value of the Hilbert transform. Finally, we resampled all signals to 1000 Hz prior to subsequent analyses.

Separately from SEEG data, we also derived EMG activity, primarily for visualization purposes. To do this, we band-pass filtered (55–145 Hz, 6th order Butterworth filter) the two EMG channels and subtracted the results from each other. For each trial, we detected the EMG onset time as the first time point where absolute EMG activity exceeded 1.5 times the average absolute value of EMG in the motion period.

For the purposes of our analyses, we defined the baseline period as the 1 s time interval at the end of the rest period before the onset of the black cross. Likewise, we defined the task period as the first 2 s of the motion period (see Fig. 1).

[3]In the calculation of the bipolar re-reference, the channels adjacent to noisy channels and closer to the top of the electrode shaft were excluded from re-referencing. In the calculation of the Laplacian re-reference, the channels adjacent to noisy channels, in either direction, were excluded from re-referencing.

2.6. Signal quality metrics

For each referencing method (i.e., monopolar reference and five re-referencing methods), we used three metrics to evaluate its influence on the signals: (1) the average correlation of the raw signals across channels; (2) the fraction of all channels that are related to the task; and (3) the variance accounted for by the task for alpha and broadband gamma power, respectively.

2.6.1. Correlation between channels—To assess signal correlations across channels, we computed the Pearson's correlation (r) between the raw signal of all pairwise channel combinations. We derived one correlation value for each trial and for each channel combination, and averaged the absolute results across all trials and then across all combinations of channels. This procedure resulted in one r value for each referencing method and each subject.

To ensure that our results were not driven by specific frequency bands, we repeated the above process for six frequency bands and their respective power: delta (0.5–4 Hz), theta (4–8 Hz), alpha (8–12 Hz), beta (12–30 Hz), gamma (30–60 Hz), and broadband gamma (60–140 Hz). To derive the signal for each band, we bandpass-filtered the raw signal using a 6th order Butterworth filter. To derive the power for each frequency band, we computed the squared absolute value of the Hilbert transform of the filtered signal.

2.6.2. Detection of task-related channels—For each subject, we then determined which channels changed their alpha or broadband gamma activity during the task compared to baseline.

We first calculated the pairwise Spearman's correlation coefficient (r) to determine the relationship of alpha/broadband gamma power with the task. To do this, separately for alpha and broadband gamma, we determined 100 median values of power for the baseline, and 100 median power values for the task, across all 100 trials, and correlated those 200 values with the baseline/task labels. We then performed a permutation test in which we randomly shuffled the task/baseline labels within each channel and calculated the corresponding random r value (Schalk et al., 2007). The randomization step was repeated 2500 times, thus generating a Gaussian distribution of 2500 surrogate r values. The computed channel r was considered statistically significant if it belonged to the 99th percentile of the Gaussian distribution ($p < 0.01$ after Bonferroni correction).

Finally, we calculated the ratio of task-related channels by dividing the number of task-related channels by the total number of all channels in that subject, resulting in one such ratio evaluation for each subject, referencing method, and alpha or broadband gamma activity.

2.6.3. Relationship of gamma and alpha power with the task—To determine how closely alpha or broadband gamma power reflected the change from baseline to the task, we calculated the coefficient of determination (R^2) for broadband gamma and alpha power and for each task-related channel (Kubanek et al., 2009; McFarland et al., 1997; Pfurtscheller et al., 2006). To support an objective comparison of these R^2 values across the

different referencing methods, we first identified the referencing method that detected the smallest ratio of task-related channels (i.e., the Laplacian method). We then calculated R^2 only for those channels for all referencing methods. The R^2 for each channel and referencing method was computed between the median broadband gamma and alpha power (averaged across trials) during the task period and the same signals during the baseline period.

3. Results

3.1. Influence of the reference on signal correlation

Different referencing methods have a substantial effect on the signal correlation across channels. Fig. 3 presents examples of signal traces for monopolar recordings (panel A) and the same recordings after Laplacian re-referencing (panel B). Using the monopolar referencing method, SEEG signals are substantially contaminated by common noise (average signal correlation across channels illustrated in Fig. 3A is 0.66). In contrast, after Laplacian re-referencing, common noise is greatly attenuated (average signal correlation across channels illustrated in Fig. 3B is 0.38), thereby revealing prominent low-frequency oscillations. In Supplementary Fig. 1, we show the difference in signal traces and the respective r for monopolar reference and the five re-referencing methods.

The important influence of referencing on common noise shown in Fig. 3 extends to other channels and all referencing methods. Fig. 4A shows the correlation matrices of all contacts in Subject 12 for all six referencing methods. By using the monopolar reference, large correlation values are evident for many pairs of channels. This correlation is reduced for GWR, CAR, ESR, and bipolar (b-e, respectively). Cross-channel correlation is almost absent for the Laplacian re-reference (f).

These observations also hold true for all subjects (Fig. 4B). Bars give the mean correlation (r) and its standard error, calculated across all channels and subjects (Section 2.6.1). The six referencing methods are ranked from worst to best as follows: monopolar reference, GWR, CAR, ESR, bipolar and Laplacian re-reference. Average cross-channel correlation is high for monopolar referencing ($r = 0.31 \pm 0.04$), and substantially reduced for Laplacian re-referencing ($r = 0.06 \pm 0.01$). The Laplacian method has a smaller cross-channel correlation than all other referencing methods ($p < 0.001$, paired t-test). We come to the same conclusion when we compute the correlations separately for task and baseline periods and for six different frequency bands (Supplementary Fig. 2).

The results presented here are consistent with the cross-channel correlations reported in Mercier et al. (2017). The reduced average correlation observed for the Laplacian method may reflect the elimination of volume conduction effects, as it has been documented for LFP recordings (Kajikawa and Schroeder, 2011; Kajikawa et al., 2017).

3.2. Influence of the reference on detection of task-related channels

The substantial inter-channel correlation shown in Figs. 3A and 4 suggests that task-related information may be erroneously induced into other channels. Thus, we next investigated the effect of the reference on the fraction of all channels that were related to the task. To do this, we obtained the ratio of both broadband gamma and alpha task-related channels for each

subject, and then averaged them across all subjects for each of the referencing method. As can be seen in Fig. 5, the monopolar reference produces the largest fraction of task-related channels (Broadband Gamma: 37.1 ± 7.4% (panel A), Alpha: 35.1 ± 9.3% (panel B)), whereas the Laplacian re-reference produces the smallest fraction (Broadband Gamma: 27.0 ± 4.7% (panel A),[4] Alpha: 22.1 ± 5.5% (panel B)). It is worth noting that the widely-used CAR method results in a larger fraction of task-related channels than does the Laplacian for both broadband gamma and alpha. Furthermore, the spatial resolution of intracranial recordings has been established to be on the order of 2 mm (Freeman et al., 2000; Slutzky et al., 2010). Thus, we deem it unlikely that the reduction of task-related channels for the Laplacian method is due to its higher spatial cutoff frequency compared to the other techniques.

3.3. Influence on the reference on relationship of broadband gamma and alpha power with the task

Finally, we are interested in determining the effect of the reference on the relationship between broadband gamma and alpha power with the task, respectively. Fig. 6 gives an example of broadband gamma signals with monopolar (panel A) referencing and Laplacian (panel B) re-referencing. The Laplacian-filtered signals in (B) are qualitatively better related to the movement. This qualitative impression is confirmed by quantitative assessment of the fraction of the broadband gamma variance that is related to the movement; average R^2 of 0.42 for monopolar referencing; average R^2 of 0.57 for Laplacian re-referencing; these R^2 values are derived only for the example channels shown in this figure. In Supplementary Fig. 3, we show examples of broadband gamma and R2 time courses for all referencing methods.

Our data demonstrate that the same observation extends to data from all channels and subjects. Fig. 7 illustrates the time courses of broadband gamma (panel A) and alpha power (panel C), averaged across all task-related channels in all subjects, as well as time courses of R_2 for broadband gamma (panel B) and alpha power (panel D), for the monopolar referencing and Laplacian re-referencing methods (red and blue traces, respectively; see Supplementary Fig. 4 for data from all referencing methods). Using the Laplacian re-reference decreases both alpha power and broadband gamma power in the entire time period (Fig. 7A and C). More importantly, using the Laplacian re-reference increases the relationship of both signals with the task (Fig. 7B and D).

To compare all referencing methods, we computed the mean R^2 value across all task-related channels from all subjects for all referencing methods. As shown in Fig. 8A, the use of the Laplacian produces substantially higher R^2 values compared to the use of the monopolar reference, for both broadband gamma (panel A) and alpha power (panel B).

4. Discussion

In this paper, we provide the first comprehensive evaluation of the effect of different referencing methods on SEEG recordings using data recorded during a motor task from 15 human subjects that were implanted with a total of 2151 electrode contacts. In our

[4]The p value for the comparison between monopolar and Laplacian in Fig. 5- A is 0.06.

evaluations, we considered the correlation of signals across channels, the fraction of channels that were related to the task, and the fraction of the variance in broadband or alpha signals that was accounted for by the task.

Our results showed that a Laplacian re-reference, i.e., re-referencing an SEEG contact against its two neighbors on the same shaft, minimizes inter-channel correlations in the SEEG time courses, minimizes the fraction of locations that appear to be related to the task for both broadband gamma and alpha power, respectively, and at the same time maximizes the relationship with the task for both broadband gamma and alpha power activity. Thus, our results support the general use of the Laplacian re-reference for pre-processing in studies of broadband gamma and low-frequency oscillatory activity in SEEG signals, which should help to facilitate the use of the emerging and unique SEEG method for exploration of neural dynamics across the entire human brain.

While our results suggest the use of the Laplacian for broadband gamma and low-frequency oscillatory activity, it may not be optimal for other purposes. For example, local re-referencing methods have been shown to introduce phase shifts or even reversals (Arnulfo et al., 2015; Shirhatti et al., 2016), which should be considered in studies in which the accuracy of phase measurements is important, such as ERP or phase synchronization analyses. Likewise, clinical use of SEEG is often focused on identifying epileptic activity using monopolar derivations, but our data do not support any conclusions about the effectiveness of the Laplacian for this purpose.

More generally, our study describes an empirical assessment of different referencing methods rather than a mathematical design of a particular referencing method based on a specific model of SEEG signals and noise. Because detailed models for these signal components do not exist, optimal referencing methods will continue to have to be evaluated empirically in the context of a specific purpose.

Supplementary Material

Refer to Web version on PubMed Central for supplementary material.

Acknowledgments

This work was supported by grants from the National Institutes of Health (P41-EB018783, P50-MH109429), US Army Research Office (W911NF-14-1-0440), Fondazione Neurone, National Natural Science Foundation of China (No. 61761166006, No. 51475292), and the Natural Science Foundation and Major Basic Research Program of Shanghai (No. 16JC1420102). We would like to thank Dr. Brendan Allison for his help editing the paper.

Appendix A. Abbreviations

CAR	Common Average Reference.
ECoG	Electrocorticography
EMG	Electromyography.
ERP	Event-related potential.

ESR	Electrode Shaft Reference.
GWR	Gray-White matter Reference.
IIR	Infinite Impulse Response.
LCD	Liquid-Crystal Display.
LFPs	Local Field Potentials.
LN	Line Noise.
MNI	Montreal Neurological Institute.
SEEG	Stereo-Electroencephalography.

References

Allen PJ, Fish DR, Smith SJM, 1992 Very high-frequency rhythmic activity during SEEG suppression in frontal lobe epilepsy. Electroencephalogr. Clin. Neurophysiol. 82 (2), 155–159. [PubMed: 1370786]

Arnulfo G, Hirvonen J, Nobili L, Palva S, Palva JM, 2015 Phase and amplitude correlations in resting-state activity in human stereotactical EEG recordings. Neuroimage 112, 114–127. [PubMed: 25721426]

Ayoubian L, Lacoma H, Gotman J, 2010 Automatic seizure detection in SEEG using high frequency activities in wavelet domain. Med. Eng. Phys 35 (3), 319–328.

Ball T, Kern M, Mutschler I, Aertsen A, Schulze-Bonhage A, 2009 Signal quality of simultaneously recorded invasive and non-invasive EEG. Neuroimage 46 (3), 708–716. [PubMed: 19264143]

Bancaud J, Talairach J, 1965 La Stéréo-électroencéphalographie Dans L'épilepsie: Informations Neurophysiopathologiques Apportées Par L'investigation Fonctionnelle Stéreotaxique. Paris: Masson.

Bancaud J, Talairach J, 1973 Methodology of stereo EEG exploration and surgical intervention in epilepsy. Rev. Oto-Neuro-Ophtalmol. (Paris) 45 (4), 315–328.

Branco M, Freudenburg Z, Aarnoutse E, Bleichner M, Vansteensel M, Ramsey N, 2017 Decoding hand gestures from primary somatosensory cortex using high-density ECoG. Neuroimage 147, 130–142. [PubMed: 27926827]

Cardinale F, Casaceli G, Raneri F, Miller J, Russo GL, 2016 Implantation of stereoelectroencephalography electrodes: a systematic review. J. Clin. Neurophysiol 33 (6), 490–502. [PubMed: 27918344]

Chabardes S, Abel TJ, Cardinale F, Kahane P, 2017 Commentary: understanding stereoelectroencephalography: what's next? Neurosurgery 82 (1), E15–E16.

Chao ZC, Nagasaka Y, Fujii N, 2010 Long-term asynchronous decoding of arm motion using electrocorticographic signals in monkey. Front. Neuroeng. 3, 3. [PubMed: 20407639]

Coon W, Gunduz A, Brunner P, Ritaccio AL, Pesaran B, Schalk G, 2016 Oscillatory phase modulates the timing of neuronal activations and resulting behavior. Neuroimage 133, 294–301. [PubMed: 26975551]

Cossu M, Cardinale F, Castana L, Citterio A, Francione S, Tassi L, Benabid AL, Lo Russo G, 2005 Stereoelectroencephalography in the presurgical evaluation of focal epilepsy: a retrospective analysis of 215 procedures. Neurosurgery 57 (4), 706–718 discussion 706–18. [PubMed: 16239883]

Desikan RS, Ségonne F, Fischl B, Quinn BT, Dickerson BC, Blacker D, Buckner RL, Dale AM, Maguire RP, Hyman BT, Albert MS, Killiany RJ, 2006 An automated labeling system for subdividing the human cerebral cortex on MRI scans into gyral based regions of interest. Neuroimage 31 (3), 968–980. [PubMed: 16530430]

Fischl B, Salat DH, Busa E, Albert M, Dieterich M, Haselgrove C, van der Kouwe A, Killiany R, Kennedy D, Klaveness S, Montillo A, Makris N, Rosen B, Dale AM, 2002 Whole brain segmentation. Neuron 33 (3), 341–355. [PubMed: 11832223]

Freeman WJ, Rogers LJ, Holmes MD, Silbergeld DL, 2000 Spatial spectral analysis of human electrocorticograms including the alpha and gamma bands. J. Neurosci. Meth 95 (2), 111–121.

Gaona CM, Sharma M, Freudenburg ZV, Breshears JD, Bundy DT, Roland J, Barbour DL, Schalk G, Leuthardt EC, 2011 Nonuniform high-gamma (60-500 Hz) power changes dissociate cognitive task and anatomy in human cortex. J. Neurosci 31 (6), 2091–2100. [PubMed: 21307246]

Guenot M, Isnard J, Ryvlin P, Fischer C, Ostrowsky K, Mauguiere F, Sindou M, 2001 Neurophysiological monitoring for epilepsy surgery: the Talairach SEEG method. Stereotact. Funct. Neurosurg 77 (1–4), 29–32. [PubMed: 12378053]

Haegens S, Nacher V, Luna R, Romo R, Jensen O, 2011 alpha-oscillations in the monkey sensorimotor network influence discrimination performance by rhythmical inhibition of neuronal spiking. Proc. Natl. Acad. Sci. Unit. States Am 108 (48), 19377–19382.

He BJ, Snyder AZ, Zempel JM, Smyth MD, Raichle ME, 2008 Electrophysiological correlates of the brain's intrinsic large-scale functional architecture. Proc. Natl. Acad. Sci. Unit. States Am 105 (41), 16039.

Jensen O, Mazaheri A, 2010 Shaping functional architecture by oscillatory alpha activity: gating by inhibition. Front. Hum. Neurosci 4, 186. [PubMed: 21119777]

Jerbi K, Ossandon T, Hamame CM, Senova S, Dalal SS, Jung J, Minotti L, Bertrand O, Berthoz A, Kahane P, Lachaux JP, 2009 Task-related gamma-band dynamics from an intracerebral perspective: review and implications for surface EEG and MEG. Hum. Brain Mapp 30 (6), 1758–1771. [PubMed: 19343801]

Kajikawa Y, Schroeder C, 2011 How local is the local field potential? Neuron 72 (5), 847–858. [PubMed: 22153379]

Kajikawa Y, Smiley J, Schroeder C, 2017 Primary generators of visually evoked field potentials recorded in the macaque auditory cortex. J. Neurosci 37 (42), 10139–10153. [PubMed: 28924008]

Klimesch W, 2012 Alpha-band oscillations, attention, and controlled access to stored information. Trends Cognit. Sci 16 (12), 606–617. [PubMed: 23141428]

Kobayashi K, Jacobs J, Gotman J, 2009 Detection of changes of high-frequency activity by statistical time-frequency analysis in epileptic spikes. Clin. Neurophysiol 120 (6), 1070–1077. [PubMed: 19394892]

Koessler L, Benar C, Maillard L, Badier JM, Vignal JP, Bartolomei F, Chauvel P, Gavaret M, 2010 Source localization of ictal epileptic activity investigated by high resolution EEG and validated by SEEG. Neuroimage 51 (2), 642–653. [PubMed: 20206700]

Kubanek J, Miller KJ, Ojemann JG, Wolpaw JR, Schalk G, 2009 Decoding flexion of individual fingers using electrocorticographic signals in humans. J. Neural. Eng 6 (6), 066001. [PubMed: 19794237]

Kubanek J, Schalk G, 2015 NeuralAct: a tool to visualize electrocortical (ECoG) activity on a three-dimensional model of the cortex. Neuroinformatics 13 (2), 167–174. [PubMed: 25381641]

Lachaux JP, Hoffmann D, Minotti L, Berthoz A, Kahane P, 2006 Intracerebral dynamics of saccade generation in the human frontal eye field and supplementary eye field. Neuroimage 30 (4), 1302–1312. [PubMed: 16412667]

Lachaux JP, Rudrauf D, Kahane P, 2003 Intracranial EEG and human brain mapping. J. Physiol. Paris 97 (4), 613–628. [PubMed: 15242670]

Lakatos P, Chen CM, O'Connell MN, Mills A, Schroeder CE, 2007 Neuronal oscillations and multisensory interaction in primary auditory cortex. Neuron 53 (2), 279–292. [PubMed: 17224408]

Landré E, Chipaux M, Maillard L, Szurhaj W, Trebuchon A, 2018 Electrophysiological technical procedures. Neurophysiol. Clin 48 (1), 47–52. [PubMed: 29254834]

Lang Michael J., Chitale ASAWC, 2016 Advancements in stereotactic epilepsy surgery: stereo-EEG laser interstitial thermotherapy and responsive neurostimulation. JHN Journal 11 (2), 32–36.

Leuthardt EC, Schalk G, Wolpaw JR, Ojemann JG, Moran DW, 2004 A brain–computer interface using electrocorticographic signals in humans. J. Neural. Eng 1 (2), 63. [PubMed: 15876624]

Liu Y, Coon W, de Pesters A, Brunner P, Schalk G, 2015 The effects of spatial filtering and artifacts on electrocorticographic signals. J. Neural. Eng 12 (5), 056008. [PubMed: 26268446]

McFarland DJ, McCane LM, David SV, Wolpaw JR, 1997 Spatial filter selection for EEG-based communication. Electroencephalogr. Clin. Neurophysiol 103 (3), 386–394. [PubMed: 9305287]

Mercier MR, Bickel S, Megevand P, Groppe DM, Schroeder CE, Mehta AD, Lado FA, 2017 Evaluation of cortical local field potential diffusion in stereotactic electro-encephalography recordings: a glimpse on white matter signal. Neuroimage 147, 219–232. [PubMed: 27554533]

Miller K, Honey C, Hermes D, Rao R, denNijs M, Ojemann J, 2014 Broadband changes in the cortical surface potential track activation of functionally diverse neuronal populations. Neuroimage 85 (2), 711–720. [PubMed: 24018305]

Munari C, Hoffmann D, Fracione S, Kahane P, Tassi L, Russo GL, Benabid AL, 1994 Stereo-electroencephalography methodology: advantages and limits. Acta Neurol. Scand 89 (S152), 56–67. [PubMed: 8178630]

Nunez PL, Westdorp AF, 1994 The surface laplacian, high resolution EEG and controversies. Brain Topogr. 6 (3), 221–226. [PubMed: 8204409]

Nurse ES, John SE, Freestone DR, Oxley TJ, Ung H, Berkovic SF, O'Brien TJ, Cook MJ, Grayden DB, 2018 Consistency of long-term subdural electrocorticography in humans. IEEE Trans. Biomed. Eng 65 (2), 344–352. [PubMed: 29364119]

Perrone-Bertolotti M, Kujala J, Vidal JR, Hamame CM, Ossandon T, Bertrand O, Minotti L, Kahane P, Jerbi K, Lachaux JP, 2012 How silent is silent reading? Intracerebral evidence for top-down activation of temporal voice areas during reading. J. Neurosci 32 (49), 17554–17562. [PubMed: 23223279]

de Pesters A, Coon WG, Brunner P, Gunduz A, Ritaccio AL, Brunet NM, de Weerd P, Roberts MJ, Oostenveld R, Fries P, Schalk G, 2016 Alpha power indexes task-related networks on large and small scales: a multimodal ECoG study in humans and a non-human primate. Neuroimage 134, 122–131. [PubMed: 27057960]

Pfurtscheller G, Brunner C, Schlögl A, Lopes da Silva FH, 2006 Mu rhythm (de) synchronization and EEG single-trial classification of different motor imagery tasks. Neuroimage 31 (1), 153–159. [PubMed: 16443377]

Potes C, Brunner P, Gunduz A, Knight RT, Schalk G, 2014 Spatial and temporal relationships of electrocorticographic alpha and gamma activity during auditory processing. Neuroimage 97, 188–195. [PubMed: 24768933]

Proserpio P, Cossu M, Francione S, Tassi L, Mai R, Didato G, Castana L, Cardinale F, Sartori I, Gozzo F, Citterio A, Schiariti M, Lo Russo G, Nobili L, 2011 Insular-opercular seizures manifesting with sleep-related paroxysmal motor behaviors: a stereo-EEG study. Epilepsia 52 (10), 1781–1791. [PubMed: 21883183]

Ray S, Maunsell JH, 2011 Different origins of gamma rhythm and high-gamma activity in macaque visual cortex. PLoS Biol. 9 (4), e1000610. [PubMed: 21532743]

Rektor I, Kanovsky P, Bares M, Brazdil M, Streitova H, Klajblova H, Kuba R, Daniel P, 2003 A SEEG study of ERP in motor and premotor cortices and in the basal ganglia. Clin. Neurophysiol 114 (3), 463–471. [PubMed: 12705427]

Rektor I, Kanovsky P, Bares M, Louvel J, Lamarche M, 2001 Event-related potentials, CNV, readiness potential, and movement accompanying potential recorded from posterior thalamus in human subjects. A SEEG study. Neurophysiol. Clin 31 (4), 253–261. [PubMed: 11596532]

Ryvlin P, Picard F, 2017 Invasive investigation of insular cortex epilepsy. J. Clin. Neurophysiol 34 (4).

Schalk G, 2010 Can electrocorticography (ECoG) support robust and powerful brain-computer interfaces? Front. Neuroeng 3, 9. [PubMed: 20631853]

Schalk G, 2015 A general framework for dynamic cortical function: the function-through-biased-oscillations (FBO) hypothesis. Front. Hum. Neurosci 9, 352. [PubMed: 26136676]

Schalk G, Kubanek J, Miller K, Anderson N, Leuthardt E, Ojemann J, Limbrick D, Moran D, Gerhardt L, Wolpaw J, 2007 Decoding two-dimensional movement trajectories using electrocorticographic signals in humans. J. Neural. Eng 4 (3), 264. [PubMed: 17873429]

Schalk G, Marple J, Knight RT, Coon WG, 2017 Instantaneous voltage as an alternative to power-and phase-based interpretation of oscillatory brain activity. Neuroimage 157, 545–554. [PubMed: 28624646]

Shirhatti V, Borthakur A, Ray S, 2016 Effect of reference scheme on power and phase of the local field potential. Neural Comput. 28 (5), 882–913. [PubMed: 26942748]

Slutzky MW, Jordan LR, Krieg T, Chen M, Mogul DJ, Miller LE, 2010 Optimal spacing of surface electrode arrays for brain–machine interface applications. J. Neural. Eng 7 (2), 026004.

Sperling MR, Connor MJ, 1989 Comparison of depth and subdural electrodes in recording temporal lobe seizures. Neurology 39 (11), 1497. [PubMed: 2812330]

Ung H, Baldassano SN, Bink H, Krieger AM, Williams S, Vitale F, Wu C, Freestone D, Nurse E, Leyde K, et al., 2017 Intracranial EEG fluctuates over months after implanting electrodes in human brain. J. Neural. Eng 14 (5), 056011. [PubMed: 28862995]

Urrestarazu E, Chander R, Dubeau F, Gotman J, 2007 Interictal high-frequency oscillations (100-500 Hz) in the intracerebral EEG of epileptic patients. Brain 130 (9), 2354–2366. [PubMed: 17626037]

Vidal JR, Freyermuth S, Jerbi K, Hamame CM, Ossandon T, Bertrand O, Minotti L, Kahane P, Berthoz A, Lachaux JP, 2012 Long-distance amplitude correlations in the high gamma band reveal segregation and integration within the reading network. J. Neurosci 32 (19), 6421–6434. [PubMed: 22573665]

Zaveri HP, Duckrow RB, Spencer SS, 2006 On the use of bipolar montages for time-series analysis of intracranial electroencephalograms. Clin. Neurophysiol 117 (9), 2102–2108. [PubMed: 16887380]

Zhang H, Jacobs J, 2015 Traveling theta waves in the human hippocampus. J. Neurosci 35 (36), 12477–12487. [PubMed: 26354915]

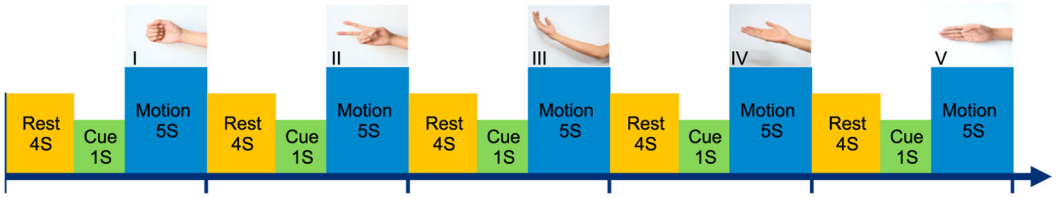

Fig. 1.

Experimental protocol. Each subject performed five different types of hand or arm movements. They performed each type of movement 20 times (5 s each). Prior to each movement, each subject rested for 4 s and then a cue (duration of 1 s) prepared the subject for movement initiation.

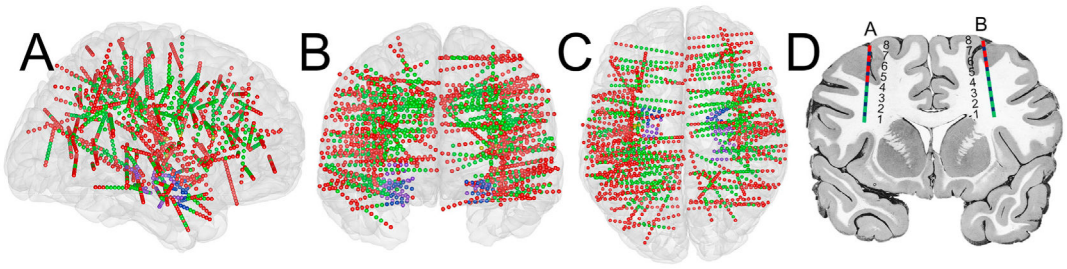

Fig. 2.

Electrode locations projected on the three-dimensional standard Montreal Neurological Institute (MNI) brain model. Panels **A**, **B**, and **C** show the brain model and implanted contacts (small colored dots) in a sagittal, coronal, and transverse view, respectively. SEEG contacts are colored differently to represent the anatomical location of each contact: red for gray matter, green for white matter, purple for hippocampus, blue for amygdala, and yellow for putamen. In total, there were 161 electrode shafts with 2151 contacts. **(D)** Example illustration of two electrode shafts that penetrate gray matter (red dots) and white matter (green dots). Each of these shafts contains 8 contacts (named A and B, respectively), and the numbers beside each electrode indicate the numerical order of contacts.

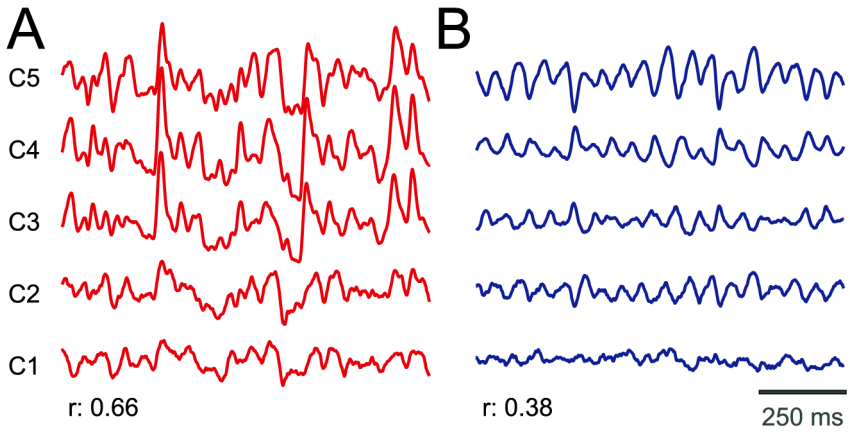

Fig. 3.

Illustration of the difference in common noise for signals with monopolar **(A)** and Laplacian **(B)** (re-)reference. Traces give SEEG time courses for five example channels from Subject 1. The mean inter-channel correlation coefficient (*r*) is shown for each referencing method.

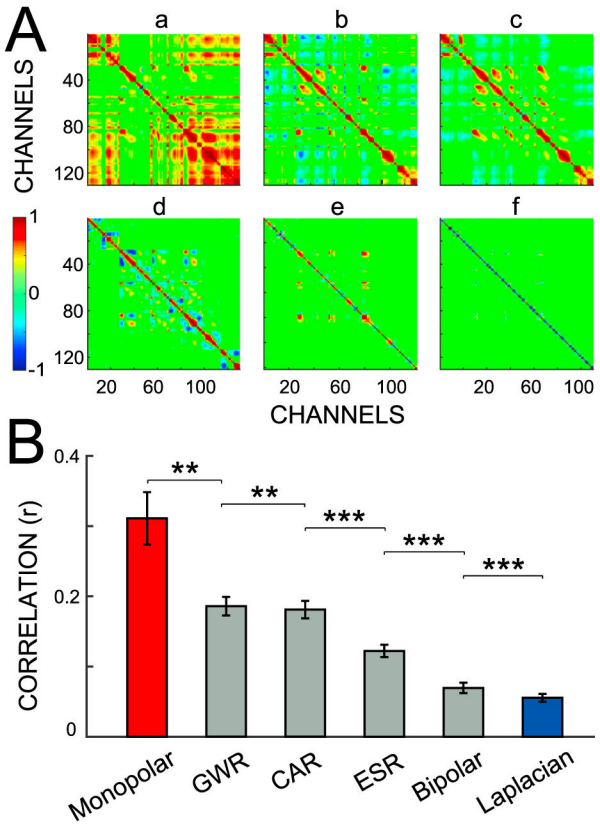

Fig. 4.

Signal correlation for different referencing methods. **(A)** Correlation matrix from Subject 12 for the six referencing methods: (a) monopolar; (b) GWR; (c) CAR; (d) ESR; (e) bipolar; and (f) Laplacian. Colors correspond to the correlation between two specific channels. The correlation between channels varies across the methods. **(B)** Average Pearson's correlation and standard error for the six referencing methods. Asterisks denote the significance of the difference between correlations established using paired t-tests: *** ($p < 0.001$), ** ($p < 0.01$). These statistical results are shown only for the nearest pairs that show a significant difference.

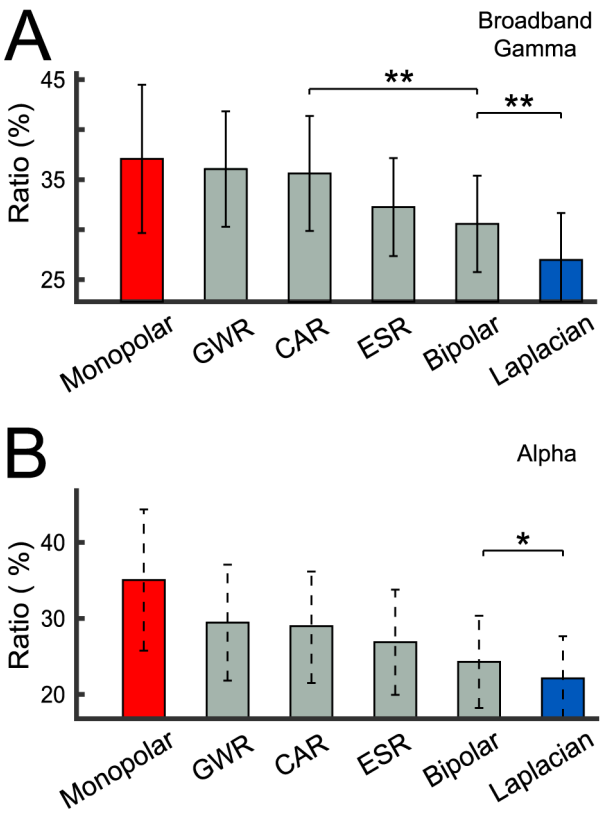

Fig. 5.

Fraction of all channels that are related to the task for different referencing methods. For each subject, we calculated the ratio of task-related channels by dividing the number of task-related channels by the number of all channels. **(A)** Mean (averaged across subjects) and standard error of the ratio of task-related channels for broadband gamma power. **(B)** Mean (averaged across subjects) and standard error of the ratio of task-related channels for alpha power. Asterisks denote the significance of the difference between the ratio of task-related channels for adjacent referencing methods, established using paired t-tests: ** ($p < 0.01$), * ($p < 0.05$). These statistical results are shown only for the nearest pairs that show a significant difference.

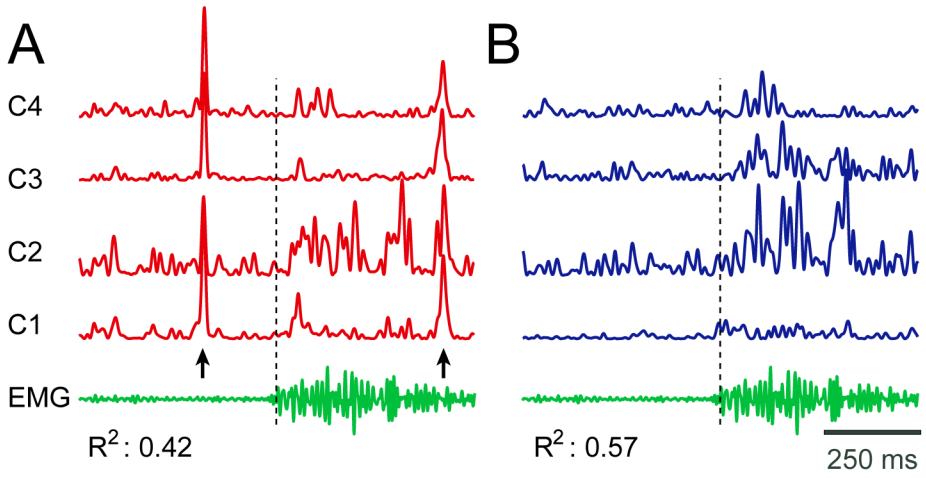

Fig. 6.

Example of broadband gamma activity for different referencing methods for four channels in Subject 8. **(A)** Broadband gamma power using monopolar reference (red traces). **(B)** Broadband gamma power using Laplacian re-reference (blue traces). The EMG signal during the same trial is also shown (green trace). The black dashed line indicates EMG onset. Arrows indicate the times of substantial artifacts in (A) that are practically absent in (B). The variance of broadband gamma accounted for by the EMG activity (R^2) is shown below the traces, and increases substantially for Laplacian re-referencing.

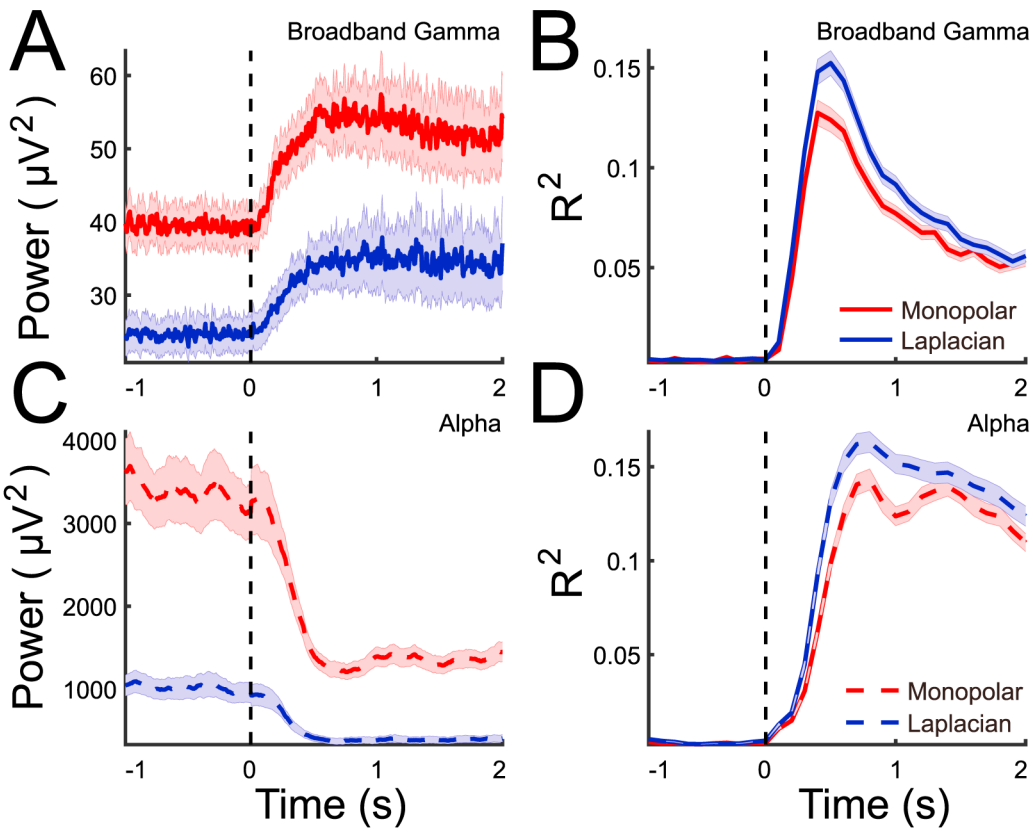

Fig. 7.

Time series of broadband gamma and alpha power and R^2 using two different referencing methods. **(A/C)**: Trial-channel averaged broadband gamma (A) and alpha power (C) across all task-related channels. Red/blue traces show results for monopolar and Laplacian methods, respectively. Shaded areas give the standard error of the mean. −1 to 0 s and 0–2 s in the figure correspond to the baseline and task period in each trial. The blacked dash line indicates the onset of movement cue. Only the signals with monopolar and Laplacian re-reference are presented. **(B/D)**. For each task-related channel, the entire time period (as presented) is binned in 100 ms segments and for each segment R^2 is calculated between broadband gamma/alpha power during that time segment and baseline. The mean (averaged across all channels and subjects) and standard error (shaded area) are shown.

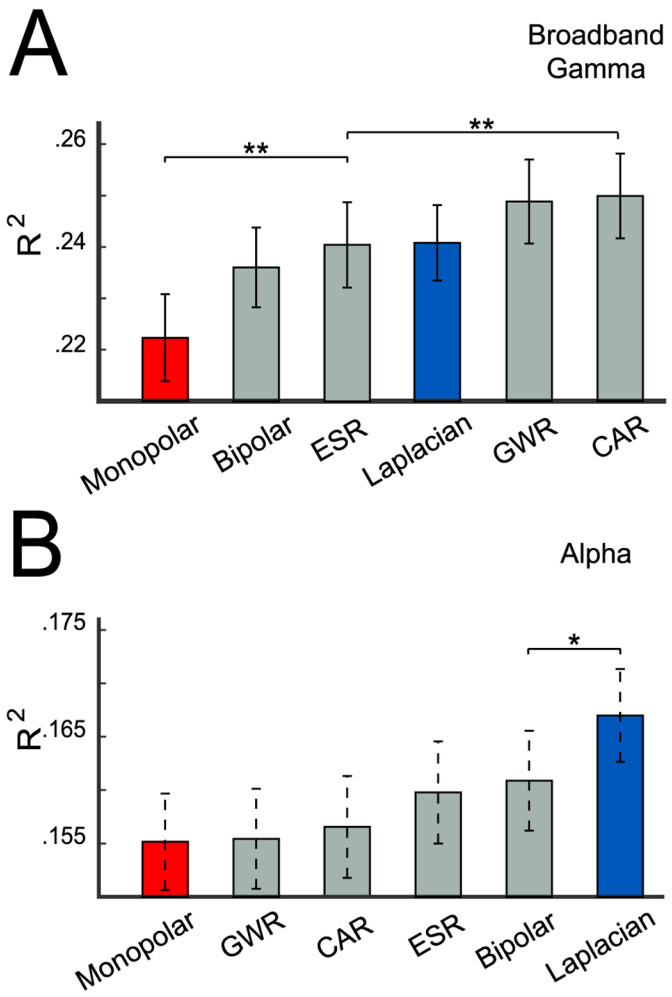

Fig. 8.

Coefficient of determination (R^2) for different referencing methods. **(A)** Mean and standard error of R^2 for broadband gamma power, calculated across all channels from all subjects. **(B)** Mean and standard error of R^2 for alpha power. Asterisks denote significance of the difference (paired t-test) between R^2 values for referencing methods: ** ($p < 0.01$), * ($p < 0.05$). These statistical results are shown only for the nearest pairs that show a significant difference.

Table 1

Clinical profiles of subjects that participated in the study.

ID	EZ	Gender	Age	RS	SR (Hz)	EL	CH
1	left posterior inferior frontal gyrus	M	23	Left	1000	10	121
2	left occipital lobe	M	33	Left	1000	15	180
3	right central region	F	30	Right	1000	7	60
4	right temporal lobe	M	26	Right	1000	13	178
5	right inferior frontal gyrus	M	25	Right	1000	10	143
6	right temporal and insular lobe	F	17	Bilateral	1000	13	169
7	right frontal lobe	F	28	Right	1000	9	114
8	left temporal parietal lobe	M	27	Left	2000	16	208
9	basal area of right temporal lobe	M	15	Bilateral	500	13	194
10	right superior parietal lobule	M	31	Right	500	6	94
11	mesial part of left frontal lobe	F	22	Left	2000	7	102
12	right anterior cingulate cortex	M	19	Bilateral	2000	9	130
13	left temporal and insular lobe	F	30	Bilateral	2000	13	170
14	left temporal lobe	M	31	Left	2000	10	144
15	left occipital and parietal lobe	M	27	Bilateral	2000	10	144

Abbreviations for this Table: EZ, Epileptogenic Zone; RS, Recording Hemisphere; SR, Sampling Rate; EL, Number of Electrode Shafts; CH: Number of Contacts.

Table 2

Definition of the contact population used for referencing.

Method	S_i	Group Used for Reference
monopolar	S_i	2 contacts in white matter
CAR	S_i	all contacts
GWR	S_i	all contacts in GM if i in GM all contacts in WM if i in WM
ESR	S_i	contacts from the el. shaft where i located
bipolar	S_{i+1}	S_i, in same el. shaft
Laplacian	S_i	2 adjacent contacts in same el. shaft (i.e., S_{i+1} and S_{i-1})

i: contact being (re-)referenced.

GM: gray matter, WM: white matter.